Article

Soledge2D-Eirene simulations of the Pilot-PSI linear plasma device compared to experimental data

K. Jesko*,[1,2] Y. Marandet,[3] H. Bufferand,[1] J. P. Gunn,[1] H. J. van der Meiden,[2] and G. Ciraolo[1]

[1] *CEA, IRFM, F-13108 Saint-Paul-Lez-Durance, France*
[2] *DIFFER - Dutch Institute for Fundamental Energy Research, De Zaale 20, 5612 AJ Eindhoven, the Netherlands*
[3] *Aix-Marseille Univ., CNRS, PIIM, UMR 7345, F-13397 Marseille Cedex 20, France*

Correspondence: *K. Jesko, Email: k.jesko@differ.nl

Present Address: DIFFER - Dutch Institute for Fundamental Energy Research, De Zaale 20, 5612 AJ Eindhoven, the Netherlands

Received -; Revised -; Accepted -

Abstract

Predictions for the operation of tokamak divertors are reliant on edge plasma simulations typically utilizing a fluid plasma code in combination with a Monte Carlo code for neutral species. Pilot-PSI is a linear device operating with a cascaded arc plasma source that produces plasmas comparable to those expected in the ITER divertor ($T_e \sim 1$ eV, $n_e \sim 10^{21}\mathrm{m}^{-3}$). In this study, plasma discharges in Pilot-PSI have been modelled using the Soledge2D fluid plasma code [1] coupled to the Eirene neutral Monte Carlo code. The plasma is generated using an external source of plasma density and power. These input parameters are tuned in order to match Thomson scattering (TS) measurements close to the cascaded arc source nozzle. The sensitivity of the simulations to different atomic physics models was explored. It was found that elastic collisions between ions and hydrogen molecules have a strong influence on calculated profiles. Without their inclusion, supersonic flow regimes are obtained with M ~ 2 close to the target plate. Simulation results have been compared with experimental findings using TS close to the target and in the case of Pilot-PSI, a Langmuir probe embedded in the target. Comparison between experimental trends observed in a background pressure scan [2] and the simulations show that the inclusion of the elastic collision is mandatory for the trends to be reproduced.

Keywords: linear plasma device, detachment, divertor, Soledge2D-Eirene

1 Introduction

The technological limit of steady-state power loading of the ITER plasma-facing components (PFCs) is 10 MW/m^2 [3]. The plasma heat flux to the PFCs is chanelled through a narrow layer given by the power flux fall-off length, λ_q. The numerical value of this parameter has been extrapolated to ITER using multi-machine scaling [4] and has a pessimistic value of ~ 1 mm. Therefore, in order to avoid excessive heating of the PFCs, a large fraction of the plasma

heat flux has to be dissipated before reaching the divertor targets. This can be achieved by radiation of a significant amount of power by impurity species and/or by transferring the plasma kinetic energy to neutral hydrogen particles (e.g. via excitation, charge-exchange) which are inherently present in the vicinity of the plasma-solid interface. Neither photons nor neutral particles follow magnetic field lines and can potentially spread the heat load over a larger area of the PFCs. Additionally, these processes can lead to detached divertor regimes, where significant reduction of power and particle fluxes can occur between upstream and target locations. For ITER and next step fusion facilities, predictions of heat and particle transport from upstream locations of the scrape-off layer to the PFCs rely largely on modelling using fluid/Monte Carlo code packages (i.e. SOLPS, SolEdge2D-Eirene, EDGE2D-Eirene, SOLDOR/NEUT2D). Within this work, we use the SolEdge2D-Eirene code to simulate the Pilot-PSI linear plasma device. Pilot-PSI offers a high density ($n_e \sim 10^{20} - 10^{21}$ m^{-3}), low temperature ($T_e \sim 0.1$ - 5 eV) plasma relevant to detached divertors. The simulations are compared to experimental data published in [2]. Such an approach enables to 1) provide interpretation for the experimental results by detailed bookkeeping of individual processes within the code, 2) assess how accurately the code can reproduce experimental findings with implications for divertors and 3) point towards ways of improving the performance of linear plasma devices to deliver high power and particle fluxes for the needs of material testing.

2 The Pilot-PSI linear plasma generator

The Pilot-PSI [5] linear device uses a cascaded arc discharge source and is depicted in Fig. 1. A cylindrical r-ϕ-z coordinate system is used, where the z-coordinate is aligned with the magnetic field and is the axis of symmetry of the plasma beam and z=0 is situated at the exit of the source discharge channel. The cascaded arc operates in steady state and the discharge channel is fed by a constant gas flow rate typically in the range of 1.5 to 3.0 standard liters per minute (1 slm $\sim 4\times10^{20}$ molecules per second). The plasma leaving the arc discharge chamber is confined by an axial magnetic field that in the experiment shown here had a magnitude of 0.2T. Typical discharge currents are 100 - 220 A. The background neutral pressure in the vessel is given by the pumping and the inflow of the residual neutrals from the source and is typically of the order of several Pa. The plasma beam is terminated at axial position z=56 cm by an actively cooled solid target. The key diagnostic was Thomson scattering which was performed at two axial locations (at z=4 cm and z=54 cm, referred to as "upstream" and "target" locations, respectively) and is particularly suited to measure low temperature plasmas in the range 0.07 eV to 5.0 eV [6]. A single Langmuir probe was embedded in the target with a collecting area perpendicular to the magnetic field lines. The current collecting surface was circular and 2 mm in diameter. The backround neutral pressure, which we will denote as P_n, was measured by a capacitance manometer.

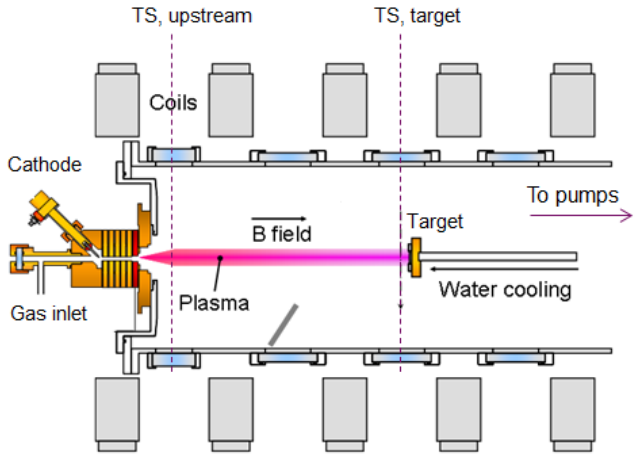

Figure 1: Schematic layout of the Pilot-PSI linear plasma device, with the two positions where radial profile measurements using Thomson scattering can be performed.

3 Simulation setup

The Soledge2D transport code was designed for investigation of the transport of quasineutral plasma in the tokamak edge plasma and in the SOL [1, 7] and is coupled to the kinetic Monte-Carlo (MC) code Eirene [8]. The code assumes toroidal symmetry. The equations for density, parallel velocity and electron and ion temperature are solved. The parallel transport is solved self-consistently while the cross-field transport is imposed by ad-hoc diffusion coefficients. Kinetic corrections for cases with low collisionality are provided by the use an artificial flux limiter. Drifts, electric fields and currents are implemented in Soledge2D [9], however they were turned off in simulations presented in this contribution.

The geometry of the linear plasma device may seem very different from a tokamak, however they have common aspects, which enable to create a field-aligned grid that the code can directly use. The grid for the linear device can be regarded as a subspace of a tokamak grid. It is in fact topologically equivalent to a scrape-off layer with no toroidal field and no major radius, i.e. the plasma is simulated up to the axis of symmetry, unlike tokamaks. The axial magnetic field of the linear device corresponds to the poloidal magnetic field of a tokamak and had a constant value of 0.2 T in all simulations presented here, in line with the experiment. The grid used in the simulations is depicted in Fig. 2. Additionally, a variable grid density is used in order to provide high resolution in the plasma beam and close to the walls, while in areas of less interest the cells are larger, to save computational time.

The plasma wall interaction is treated using the penalization technique [10] which recovers standard Bohm boundary conditions and sheath heat transmission at the plasma-wall interface, i.e. $|M| \geq 1$ and $q_{t,\alpha} = \gamma_\alpha n M c_s T_\alpha$, where M is the Mach number, $q_{t,\alpha}$ is the energy flux density through the interface for species α (electrons or ions), c_s is the sound speed and γ_α are the sheath heat transmission factors for ions and electrons, set to 2.5 and 4.5 , respectively. The Soledge2D energy equations are written in terms of the total energy. However, the values of heat transmission factors

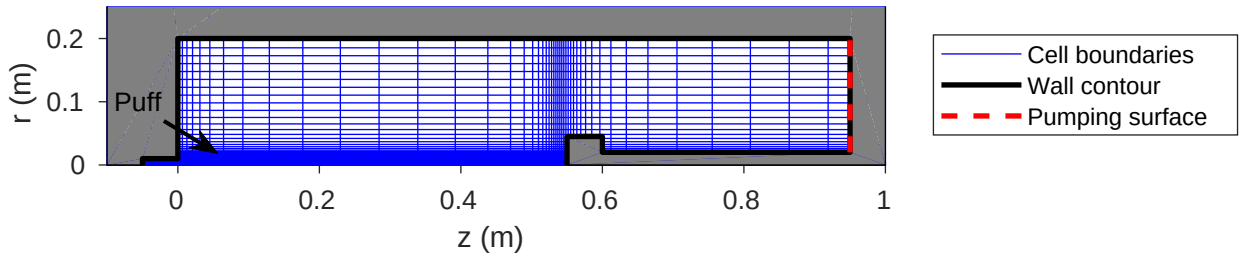

Figure 2: The Pilot-PSI non-uniform grid used in the Soledge2D-Eirene simulations.

reported here are for the internal energy part. We assume the ion velocity distribution function at the sheath edge to be a shifted Maxwellian with c_s normal to the wall, so the effective sheath heat transmission factor for ions is in fact 3.5 for $T_i = T_e$. This choice ensures internal consistency of the code and is related to the coupling of SolEdge2D and Eirene. On the axis of symmetry the boundary condition of vanishing perpendicular gradients is used.

Anomalous values are assigned to the radial transport coefficients. For density, a diffusion coefficient of $D_i = 0.3$ m^2/s is chosen based on an estimate obtained from the Bohm diffusion coefficient for T_e=1 eV and B =0.2 T and is found to reproduce broadening of beam profiles at least qualitatively, Fig. 5 (D). Simulation results were found not to be sensitive to the radial thermal conductivities in the range 0.1 - 3.0 m^2/s. In the simulations, values of $\chi_{\perp}^{e,i} =$ 0.3 m^2/s are used.

It is beyond the scope of this contribution to model the details of the cascaded arc discharge self-consistently. This would require inclusion of the electric currents and drifts in the simulations, as well as thermionic emission from the hot cathode. However, the principal focus here lies in the interaction of the plasma beam with the surrounding neutral gas. Therefore, the plasma particle and power sources are directly prescribed as external volumetric source terms in the Soledge2D equations. The shape and magnitude of these is defined to match Thomson scattering profiles measured close to the source. For example, the external volumetric source terms for the plasma ion/electron source has the form of a Gaussian function in both r and z directions:

$$S_n^{(ext)}(r,z) = \frac{S_n^{(ext,tot)}}{C} \exp\Big(-(r-r_{src})^2/\lambda_r^2 \Big) \exp\Big(-(z-z_{src})^2/\lambda_z^2 \Big), \tag{1}$$

where r_{src}, z_{src} are the positions of the profile maxima, λ_r, λ_z are the profile widths, C is a normalization constant such that the volume integral over the simulation domain be equal to the total number of injected particles, i.e. $\int_V S_n^{ext} \mathrm{d}V = S_n^{ext,tot}$. The position and spatial extent of the external volumetric source terms was chosen such that it stays well within the small area of the cascaded arc source, i.e. $r_{src} = 0$, z_{src} =-2.5 cm, $\lambda_r = 0.5$ cm, $\lambda_z = 1$ cm, Fig. 2.

Table 1: List of atomic and molecular physics processes used in Eirene, listed for both AM1 and AM2. In AM1, rate coefficients for reactions (3)-(10) originate from the HYDHEL database (the remaining ones are from AMJUEL, while in AM2 all reactions are taken from the AMJUEL database. Both databases available from www.eirene.de.

#	Reaction	AM1	AM2	Event type
(1)	$H + e \rightarrow H^+ + 2e$	yes	yes	Electron impact ionization
(2)	$H + H^+ \rightarrow H^+ + H$	yes	yes	Charge exchange
(3)	$H_2 + e \rightarrow H_2^+ + + 2e$	yes	yes	Electron impact ionization
(4)	$H_2 + e \rightarrow 2H + e$	yes	yes	Dissociation
(5)	$H_2 + e \rightarrow H + H^+ + 2e$	yes	yes	Dissociative ionization
(6)	$H_2 + H^+ \rightarrow H_2 + H^+$	**n/a**	yes	Elastic collision
(7)	$H_2 + H^+ \rightarrow H_2^+ + H$	**n/a**	yes	Ion conversion
(8)	$H_2^+ + e \rightarrow H^+ + H + 2e$	yes	yes	Dissociation
(9)	$H_2^+ + e \rightarrow H^+ + H^+ + e$	yes	yes	Dissociative ionization
(10)	$H_2^+ + e \rightarrow 2H$	yes	yes	Dissociative recombination
(11)	$H^+ + e \rightarrow H$	yes	yes	Electron-ion recombination

The interaction of plasma and neutrals is handled by the Eirene Monte-Carlo code [8]. In the case of Pilot-PSI, there are three channels through which neutral particles can enter the system. 1) The constant gas flow from the cascaded arc discharge source, 2) Recycling source at the plasma wall interface and 3) Volumetric recombination. The latter two are calculated self-consistently by Eirene, while the constant gas inflow rate is simulated as a constant puff of H_2 at ambient temperature (0.03 eV) at the location depicted in Fig. 2. In the experiment, this is an externally controlable quantity and in the experiment [2] the value of the total source inflow was 2.5 standard liters per minute (slm) corresponding to about 10^{21} H_2/s in all experiments presented here. This value is also used in the simulations. The recycling coefficent at the plasma-wall interface is set to unity throughout all the simulations presented here. In order to achieve steady state a pumping surface must be present. This is located at the back end of the vessel, Fig. 2, where one can specify an absorption probability for neutral particles. The absorption probability is set to match measurements of the neutral pressure in the vacuum vessel, typically in the range of several Pa. The species considered in Eirene are hydrogen atoms H and molecules H_2 and H_2^+ molecular ions. Two different sets of atomic and molecular reactions were used in the simulations and are listed in Tab. 1. For the sake of clarity we label them AM1 and AM2. AM1 was the default set of reactions available in Eirene. AM2 corresponds to the model described in [11] (first used in [12]). However, in our case it is without neutral-neutral collisions and radiation opacity. Here, the main difference between the models is that the AM2 model contains two more reactions: elastic collisions between H^+ and H_2 and "ion conversion", which is a charge-exchange between H^+ and H_2. It was shown in [11] that the elastic collisions can affect the results significantly. Moreover, [13] also shows high sensitivity of JET detachment simulations to the atomic physics model. In the next section, a sensitivity study of simulation results involving both models and their refinements will be presented in order to determine the key processes at hand, i.e. the ones with significant effect on the solution.

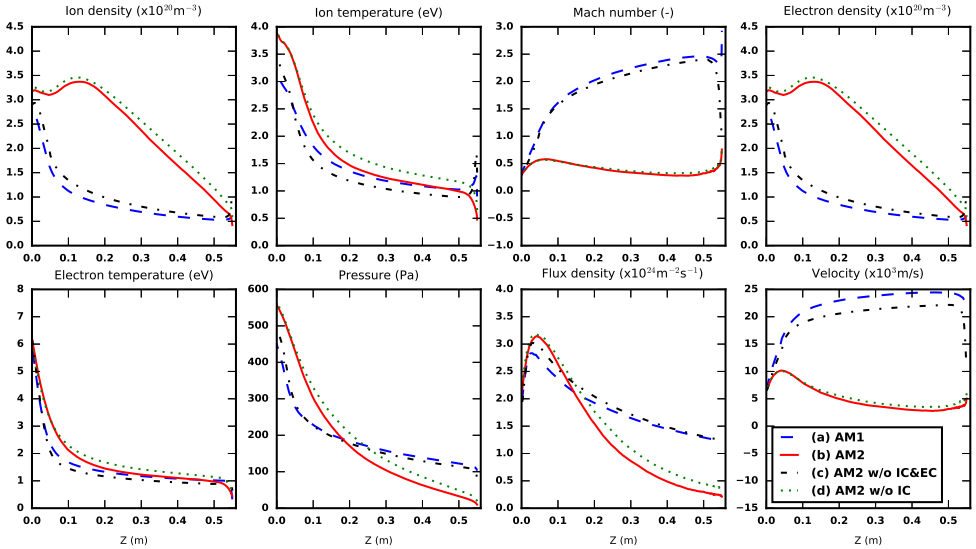

Figure 3: Parallel profiles of various plasma parameters located 1.7 mm radially from the axis of symmetry, obtained by the Soledge2D-Eirene code for different versions of the atomic physics model.

4 Results & Discussion

4.1 Impact of atomic physics on simulation results

In order to address the sensitivity of the plasma solution to the atomic physics, four different cases (a)-(d) of atomic physics reactions were used. Case (a) is the AM1 model, Case (b) is AM2, case (c) is AM2 but with the elastic collision (6), (Tab. 1) and ion conversion (7) artificially turned off (this case may seem identical to case (a), however in (a), the source database for rate coefficients for some reactions is different, see caption of Tab. 1). Lastly, case (d) is AM2 with only the ion conversion (7) turned off. For each case (a)-(d), a converged solution was obtained for a Pilot-PSI relevant plasma, with upstream n_e and T_e values of $\sim$ $3{\times}10^{20}$ m^{-3} and $\sim$ 3-5 eV. Fig. 3 shows parallel profiles of several plasma parameters for each of these four cases. The parallel profiles are taken at a radius of 1.7 mm from the axis of symmetry. It can be seen that with case (a) (AM1) the plasma enters a supersonic regime very close to the nozzle. However, in case (b) (AM2), it is found that the plasma remains subsonic. Moreover, the ion flux and plasma pressure reaching the target are also strongly reduced as opposed to case (a). The principal differences in AM1 and AM2 are the inclusion of the two processes (6), (7) in Tab. 1. In order to discriminate which of these two processes is responsible for the significant qualitative change in behavior, case (d) is introduced, where the ion conversion reaction (7) is turned off. In this case, the situation is very similar as in case (b), although some minor differences can be spotted, e.g. n_e and also the ion flux density is somewhat higher troughout the profile in case (b). Indeed, it is the elastic collisions (6) that are responsible for keeping the flow subsonic in case (b). To support this, in Fig. 4 the volumetric source terms for plasma particles, momentum and energy are plotted for the same flux

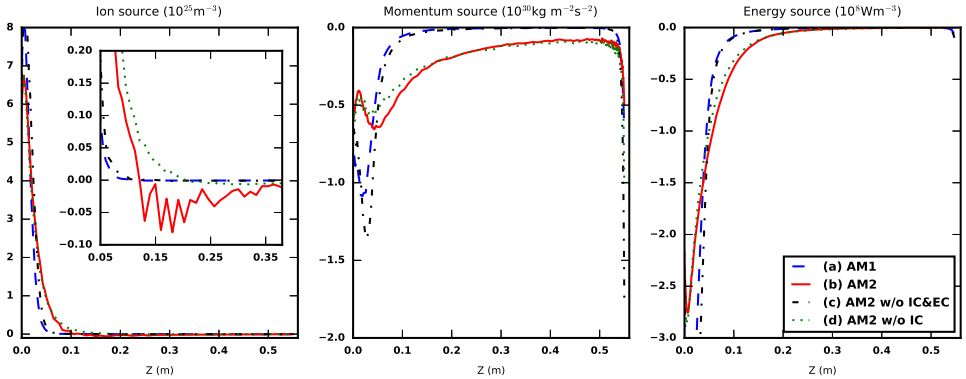

Figure 4: Parallel profiles of the plasma particle, momentum and energy sources for the field line located 1.7 mm radially from the axis of symmetry. The inset figure is a zoom-in on the particle source in the range z=0.05 m to z=0.38 m.

tube in the same color code as Fig. 3. Indeed, in case (b), a strong momentum sink appears throughout the parallel profile and is also present in case (d). Although it is known [11, 13] that the elastic collision process is important in detached/low temperature plasmas, this study illustrates the important consequences that omission of this process can have on the simulation results (e.g. by using a more crude atomic physics model).

The lower density and flux density in the case (b) as opposed to case (d) can be explained by the fact that the ion conversion reaction is the first step of the "molecular assisted recombination (MAR)" reaction chain, the second step being the dissociative recombination reaction (10). Therefore, by removing the reaction (7) the MAR pathway is now effectively forbidden in the simulations. Indeed, if one zooms in on the particle source term at the inset of Fig. 4, one can notice that for case (b) the ionization front moves closer to the cascaded arc source and that the recombination sink is much stronger as opposed to case (d) when the MAR is deactivated. On the other hand, the magnitude of the recombination is much smaller compared to ionization in both cases. It is also important to add that MAR was reported to be of large importance in linear devices [14, 15] and has triggered discussion whether it is an important recombination pathway in tokamak divertors in the past.

4.2 Comparison with experimental data

An experimental scan on the background pressure was performed, and is described in detail in [2]. Within the experiment, the pressure of the background neutral gas was changed between 3.2 Pa and 12.6 Pa by means of controlling the pumping speed. All the other input parameters were kept constant: The gas inflow rate to the cascaded arc source was 2.5 slm and the discharge current was 220A. Thomson scattering was performed at two locations of the plasma beam: 4 cm from the source nozzle and 2 cm in front of the target and a Langmuir probe was measuring the ion flux to the target. Experimentally, the plasma conditions at the source have been found to be insensitive to the background pressure [2]. In Fig. 5 (A) the ion flux density measured by the LP and recalculated from TS

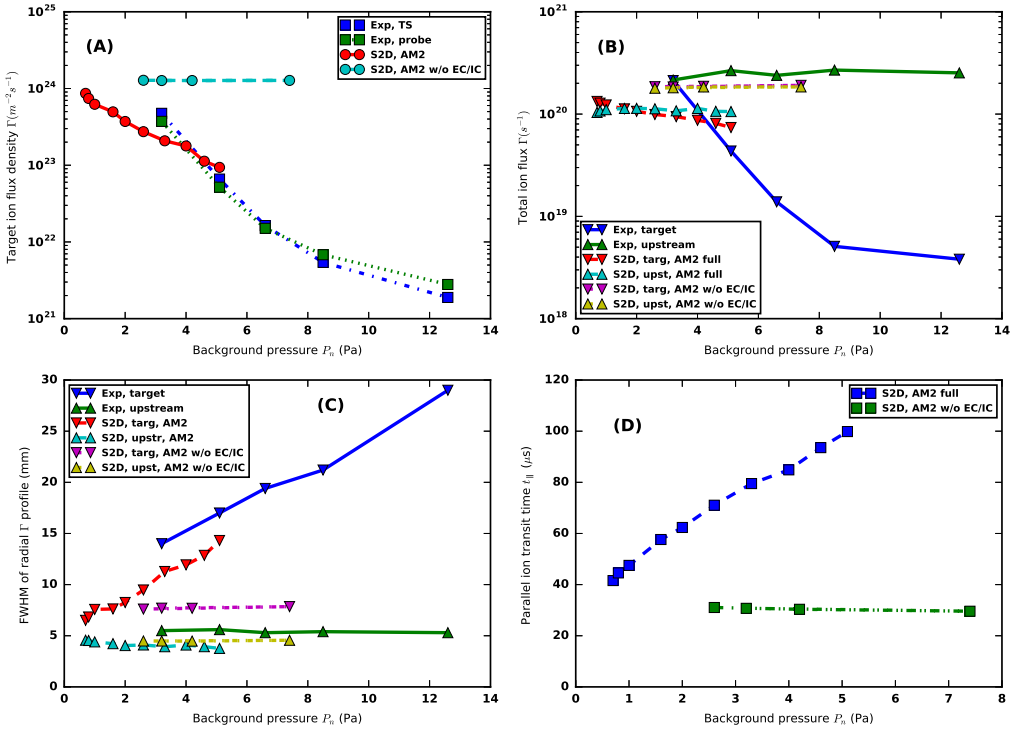

Figure 5: Comparisons between measurements of various quantities with TS and a LP and Soledge2D-Eirene simulations using different versions of the atomic physics model: (A) Target ion flux density, (B) Total, section integrated ion flux upstream and at the target, (C) FWHM of the radial ion flux density profile upstream and at the target and (D) ion transit time for two cases of the atomic physics model.

measurements at the target location are compared to values obtained from Soledge2D-Eirene. Strong reduction of the local ion flux is seen both by the LP and TS. In the simulations, the trend is recovered only with the full AM2 atomic physics model. However, the target ion flux density is completely insensitive to changes in the background pressure in the case where the ion conversion (IC) and elastic collision (EC) reactions are turned off. However, it was shown that the volume recombination sink is rather low in the simulations even with the IC included in section 4.1. The reduction in ion flux density in the simulations is caused by the radial transport: The momentum sinks caused by the EC are efficient at slowing down the plasma flow (see section 4.1). The parallel ion transit time ($\tau_{\parallel} = \int_u^t v_z^{-1} \mathrm{d}z$, where v_z is the drift velocity in the z (parallel) direction) is strongly increased, as seen in Fig. 5 (D), giving the plasma more time for perpendicular diffusion.

In Fig. 5 (C) the full width half maxima of the radial ion flux profiles $\Gamma(r)$ are plotted as a function of the P_n for both experiment and simulation. In the experiment, it can be seen that at the target, the FWHM of the Γ profile is broadening with an increase in the background pressure, while at upstream it remains constant. In the simulations this trend can only be reproduced with the full AM2 model. It is to be noted that the magnitude of the broadening

in the simulations is set by the perpendiclar diffusion coefficients. In the case of omission of the EC and IC processes a constant value of the broadening throughout the P_n scan is obtained.

Next, the total, radial section-integrated ion flux ($\Gamma_{tot}(z) = \int_S r\Gamma(r,z)\mathrm{d}r\mathrm{d}\phi = 2\pi \int_0^R r\Gamma(r,z)\mathrm{d}r$, where S is the area of the radial section of the vessel and R is the vessel radius) is plotted for both experiments and simulations. There was no measurement available to calculate the plasma velocity upstream, however, from earlier work using spectroscopy [5, 16] it can be taken that the plasma flow velocity at z=4 cm is between 2 km/s and 5 km/s for a broad range of machine settings in terms of B-field, discharge current and flow rate. A Mach number of 0.4 was assumed for all the experimental profiles in question. This assumption may seem crude, however what we are really interested in is the *reductions* of plasma flux, rather than the absolute values. As can be seen in Fig. 5 (B), the total ion flux at the target is strongly reduced with the exception of the case with the lowest background pressure, for which we cannot conclude regarding this matter. For all the other P_n cases, the strong reduction of the integrated particle flux Γ_tot translates to the fact that there has to be a net plasma sink in the volume between upstream and target. In the simulations, if the EC/IC reactions are not included, this trend is not recovered, there is no difference between the total flux at upstream and target. On the other hand, after the inclusion of these processes, a small reduction in the total ion flux is recovered in the simulations for the higher end of the P_n scan. For cases with very low background pressure, the total ion flux at the target increases compared to upstream. This means that ionization dominates over recombination in the volume between these two locations, given the higher temperature for the cases with low P_n. The low P_n cases were not accessible experimentally due to constraints of the pumping system and conversely, the high P_n cases could not be simulated due to numerical instabilities. Future work will be focused on broadening the window of overlap between measurements and simulations.

5 Conclusions

In this paper we report on Soledge2D-Eirene simulations of the Pilot-PSI linear plasma device with focus on using different atomic physics models and the sensitivity of the results to them. Subsequently, simulation results are compared to experimental data from Thomson scattering and a single Langmuir probe. The elastic collision between ions and hydrogen molecules is identified as a key player in the simulations, providing momentum sinks which keep the plasma flow subsonic as opposed to cases when the process is not included. The ion conversion reaction provides the pathway for the H_2^+ branch of molecule assisted recombination (MAR), which is the strongest recombination channel, however the total magnitude of recombination is small compared to the total ionization source. Comparison between experimental trends observed in a background pressure scan and the simulations show that the inclusion of the elastic collision is mandatory for the trends to be reproduced. This result demonstrates that it is important to use the atomic model introduced in [12] for detached/low temperature cases with high neutral molecule densities and

that using versions without elastic collisions can lead to qualitatively different simulation results. Strong reduction of the ion flux density at the target is reproduced in the simulations, however it is mainly driven by radial transport. The total volume recombination source appears to be underestimated in the simulations. However, cases with high background pressure were not accessible so far in the simulations and are subject to further study.

Acknowledgments

This work was granted access to the HPC resources of Aix-Marseille University financed by the project Equip@Meso (ANR-10-EQPX-29-01) of the program "Investissements d'Avenir" supervised by the Agence Nationale pour la Recherche. This work was carried out with financial support from NWO and was carried out within the framework of the Erasmus Mundus International Doctoral College in Fusion Science and Engineering (FUSION-DC). This work has been carried out within the framework of the EUROfusion Consortium and has received funding from the Euratom research and training programme 2014-2018 under grant agreement No 633053. The views and opinions expressed herein do not necessarily reflect those of the European Commision.

Financial disclosure

None reported.

Conflict of interest

The authors declare no potential conflict of interests.

References

[1] H. Bufferand, et al, *Nuclear Fusion* **2015**, *55*(*5*).

[2] K. Jesko, et al, *Nuclear Materials and Energy* **2017**, *12*, 1088-1093.

[3] R. A. Pitts, et al, *Physica scripta* **2009**, *T138*(*014001*).

[4] T. Eich, et al, *Physical review letters* **2011**, *107*, 215001.

[5] G. J. van Rooij, et al, *Applied physics letters* **2007**, *90*(*12*), 121501.

[6] H. J. van der Meiden, et al, *Applied physics letters* **2008**, *79*(*1*), 013505.

[7] L. Isoardi, et al, *Journal of Computational Physics* **2010**, *229*, 2220-2235.

[8] D. Reiter, et al, *Fusion Science and Technology* **2005**, *47*, 172-186.

[9] H. Bufferand, et al, *Nuclear Materials and Energy* **2017**, *12*, 852-857.

[10] H. Bufferand, et al, *Journal of Nuclear Materials* **2013**, *229*, S445-S448.

[11] V. Kotov, et al, *Plasma Physics and Controlled Fusion* **2008**, *50(10)*, 105012.

[12] A. Kukushkin, et al, *Nuclear Fusion* **2005**, *45(7)*.

[13] C. Guillemaut, et al, *Nuclear Fusion* **2014**, *54(9)*.

[14] N. Ohno, et al, *Physical Review Letters* **1998**, *81(4)*, 818-821.

[15] S. I. Krasheninnikov, et al, *Physics Letters A* **1996**, *214(5)*, 285-291.

[16] Veremiyenko V.P., *Doctoral Thesis, Technische Universiteit Eindhoven* **2006**.